

Conservation of Hamiltonian using Continuous Galerkin Petrov time discretization scheme

M. A. Qureshi¹, S. Hussain², and Ghulam Shabbir³

^{1,3}Faculty of Engineering Sciences, GIK Institute of Engineering Sciences and Technology, Topi, Khyber Pakhtunkhwa, Pakistan.

²Department of Mathematics, Mohammad Ali Jinnah University, Islamabad, Pakistan. Emails: amergikian@yahoo.com

Abstract

Continuous Galerkin Petrov time discretization scheme is tested on some Hamiltonian systems including simple harmonic oscillator, Kepler's problem with different eccentricities and molecular dynamics problem. In particular, we implement the fourth order Continuous Galerkin Petrov time discretization scheme and analyze numerically, the efficiency and conservation of Hamiltonian. A numerical comparison with some symplectic methods including Gauss implicit Runge-Kutta method and general linear method of same order is given for these systems. It is shown that the above mentioned scheme, not only preserves Hamiltonian but also uses the least CPU time compared with upto-date and optimized methods.

Mathematics Subject Classification:

Keywords: Hamiltonian systems, Continuous Galerkin Petrov time discretization, G-symplectic general linear methods, Runge-Kutta Method, Simple harmonic oscillator, Kepler's problem and Molecular dynamics problem

1 Introduction

Non-dissipative phenomena arising in the fields of classical mechanics, molecular dynamics, accelerator physics, chemistry and other sciences are modeled by Hamiltonian systems. Hamiltonian systems define equations of motion based on generalised co-ordinates $q_i = (q_1, q_2, \dots, q_n)$ and generalised momenta $p_i = (p_1, p_2, \dots, p_n)$ and are given as,

$$\frac{dp_i}{dt} = -\frac{\partial H}{\partial q_i}, \quad \frac{dq_i}{dt} = \frac{\partial H}{\partial p_i}, \quad i = 1, \dots, n, \quad (1)$$

having n degrees of freedom. $H : \mathbb{R}^{2n} \times \mathbb{R}^{2n} \rightarrow \mathbb{R}$ is the total energy of the Hamiltonian system. A separable Hamiltonian has the structure

$$H(p, q) = T(p) + V(q)$$

in mechanics, $T = \frac{1}{2}P^T M^{-1}P$ represents the kinetic energy and V being the potential energy. The Hamiltonian system in partitioned form takes the form

$$\frac{dp_i}{dt} = -\nabla_q V, \quad \frac{dq_i}{dt} = \nabla_p T = M^{-1}p.$$

The first observation is that, for autonomous Hamiltonian systems, H is an invariant, thus by differentiating $H(p, q)$ with respect to time we have,

$$\frac{dH}{dt} = \sum_{i=1}^n \left(\frac{\partial H}{\partial p_i} \frac{dp_i}{dt} + \frac{\partial H}{\partial q_i} \frac{dq_i}{dt} \right) = 0.$$

We can write $y = (p, q)$, then (1) can be written as,

$$y' = J^{-1}\nabla H,$$

where $'$ represents the derivative with respect to time, ∇ is a gradient operator and J is a skew symmetric matrix consisting of zero matrix 0 and $n \times n$ identity matrix I ,

$$J = \begin{bmatrix} 0 & I \\ -I & 0 \end{bmatrix}.$$

Another property of Hamiltonian systems is that its flow is symplectic, i.e. for a linear transformation $\Psi : \mathbb{R}^{2n} \mapsto \mathbb{R}^{2n}$, the jacobian matrix $\Psi'(y)$ satisfies

$$\Psi'^T(y)J\Psi'(y) = J.$$

Conservation laws for Hamiltonian systems are generally lost while integrating these system. It is generally desirable to preserve the underlying qualitative property of solutions of Hamiltonian systems. This is achieved by using symplectic integrators from the class of one step, multistep and general linear methods. A lot of attention has been paid on the construction and implementation of such integrators, for details see [1], [2], [3] and [4].

The continuous Galerkin Petrov time discretization scheme (cGP) was investigated in [5] for the system of ordinary differential equations (ODEs). In [6], this scheme was studied for the heat equation. In particular, the cGP(2) scheme has found to be 4th order accurate in the discrete time point and is A-stable method.

The objective of this paper is to provide analysis of cGP(2) scheme [5, 6, 7, 8] on some Hamiltonian systems and comparing it with other symplectic methods of order four including Gauss implicit Runge-Kutta method represented as irk4 [9] and a g-symplectic general linear method represented by glm4 of same order developed in [10] and [11]. In section two a brief introduction about the methods is given. The tested problems of Hamiltonian systems along with numerical experiments of these methods on Hamiltonian systems are described in third section. Conclusion based on numerical comparison of third section is given in fourth section.

2 The Methods

2.1 Continuous Galerkin-Petrov method (cGP)

As a model problem we consider the ODE system given in (1): Find $u : [0, T_m] \rightarrow W$ such that

$$\begin{aligned} d_t u(t) &= F(t, u(t)) \quad \text{for } t \in (0, T_m), \\ u(0) &= 0 \end{aligned} \quad (2)$$

The *weak formulation* of problem (2) reads: Find $u \in X$ such that $u(0) = u_0$ and

$$\int_0^{T_m} \langle d_t u(t), v(t) \rangle dt = \int_0^{T_m} \langle F(t, u(t)), v(t) \rangle dt \quad \forall v \in Y, \quad (3)$$

where X denotes the *solution space* and Y the test space. To describe the time discretization of problem (2) let us introduce the following notation. We denote by $I = [0, T_m]$ the time interval with some positive final time T_m . We start by decomposing the time interval I into N subintervals $I_n := (t_{n-1}, t_n)$, where $n \in \{1, \dots, N\}$ and

$$0 = t_0 < t_1 < \dots < t_{N-1} < t_N = T_m.$$

In our time discretization, we approximate the *continuous solution* $u(t)$ of problem (2) on each time interval I_n by a polynomial function:

$$u(t) \approx u_h(t) := \sum_{j=0}^k U_n^j \phi_{n,j}(t) \quad \forall t \in I_n, \quad (4)$$

where the "coefficients" U_n^j are elements of the Hilbert space W and the basis functions $\phi_{n,j} \in \mathbb{P}_k(I_n)$ are linearly independent elements of the standard space of polynomials on the interval I_n with a degree not larger than a given order k .

For a given time interval $J \subset \mathbb{R}$ and a Banach space B , we introduce the linear space of B -valued time polynomials with degree of at most k as

$$\mathbb{P}_k(J, B) := \left\{ u : J \rightarrow B : u(t) = \sum_{j=0}^k U^j t^j, \forall t \in J, U^j \in B, \forall j \right\}.$$

Now, the *discrete solution space* for the global approximation $u_h : I \rightarrow W$ is the space $X_h^k \subset X$ defined as

$$X_h^k := \{u \in C(I, W) : u|_{\bar{I}_n} \in \mathbb{P}_k(\bar{I}_n, W) \quad \forall n = 1, \dots, N\}$$

and the *discrete test space* is the space $Y_h^k \subset Y$ given by

$$Y_h^k := \{u \in L^2(I, W) : u|_{I_n} \in \mathbb{P}_{k-1}(I_n, W) \quad \forall n = 1, \dots, N\}.$$

The symbol h denotes the *discretization parameter* which acts in the error estimates as the maximum time step size $h := \max_{1 \leq n \leq N} h_n$, where $h_n := t_n - t_{n-1}$ is the length of the n -th time interval I_n .

Let us denote by $X_{h,0}^k := X_h^k \cap X_0$ the subspace of X_h^k with zero initial condition. Then, it is easy to see that the dimensions of the spaces $X_{h,0}^k$ and Y_h^k coincide such that it makes sense to consider the following *discontinuous*

Galerkin-Petrov discretization of order k for the weak problem (3) : Find $u_h \in u_0 + X_{h,0}^k$ such that

$$\int_0^{T_m} \langle d_t u_h(t), v_h(t) \rangle dt = \int_0^{T_m} \langle F(t, u_h(t)), v_h(t) \rangle dt \quad \forall v_h \in Y_h^k. \quad (5)$$

We will denote this discretization as the "*exact cGP(k)-method*". Since the discrete test space Y_h^k is discontinuous, problem (5) can be solved in a time marching process. Therefore, we choose test functions $v_h(t) = v\psi_{n,i}(t)$ with an arbitrary $v \in W$ and a scalar function $\psi_{n,i} : I \rightarrow \mathbb{R}$ which is zero on $I \setminus \bar{I}_n$ and a polynomial $\psi_{n,i} \in \mathbb{P}_{k-1}(\bar{I}_n)$ on the time interval $\bar{I}_n = [t_{n-1}, t_n]$. Then, we obtain for each $i = 0, \dots, k-1$

$$\int_{I_n} \langle d_t u_h(t), v \rangle \psi_{n,i}(t) dt = \int_{I_n} \langle F(t, u_h(t)), v \rangle \psi_{n,i}(t) dt \quad \forall v \in W. \quad (6)$$

By the definition of the weak time derivative we get for u_h represented by (4) the equation

$$\int_{I_n} \langle d_t u_h(t), v \rangle \psi_{n,i}(t) dt = \int_{I_n} \sum_{j=0}^k (U_n^j, v)_H \phi'_{n,j}(t) \psi_{n,i}(t) dt \quad \forall v \in W.$$

We define the basis functions $\phi_{n,j} \in \mathbb{P}_k(\bar{I}_n)$ of (4) via the reference transformation $\omega_n : \hat{I} \rightarrow \bar{I}_n$ where $\hat{I} := [-1, 1]$ and

$$t = \omega_n(\hat{t}) := \frac{t_{n-1} + t_n}{2} + \frac{h_n}{2} \hat{t} \in \bar{I}_n \quad \forall \hat{t} \in \hat{I}, n = 1, \dots, N.$$

Let $\hat{\phi}_j \in \mathbb{P}_k(\hat{I})$, $j = 0, \dots, k$, be suitable basis functions satisfying the conditions

$$\hat{\phi}_j(-1) = \delta_{0,j}, \quad \hat{\phi}_j(1) = \delta_{k,j}, \quad (7)$$

where $\delta_{k,j}$ denotes the usual Kronecker symbol. Then, we define the basis functions on the original time interval \bar{I}_n by

$$\phi_{n,j}(t) := \hat{\phi}_j(\hat{t}) \quad \text{with} \quad \hat{t} := \omega_n^{-1}(t) = \frac{2}{h_n} \left(t - \frac{t_n - t_{n-1}}{2} \right) \in \hat{I}.$$

Similarly, we define the test basis functions $\psi_{n,i}$ by suitable reference basis functions $\hat{\psi}_i \in \mathbb{P}_{k-1}(\hat{I})$, i.e.,

$$\psi_{n,i}(t) := \hat{\psi}_i(\omega_n^{-1}(t)) \quad \forall t \in \bar{I}_n, i = 0, \dots, k-1.$$

By the property (7), the initial condition and the continuity (with respect to time) of the discrete solution $u_h : I \rightarrow W$ is equivalent to the conditions:

$$U_1^0 = u_0 \quad \text{and} \quad U_n^0 = U_{n-1}^k \quad \forall n > 2.$$

We transform the integrals in (6) to the reference interval \hat{I} and obtain the following system of equations for the "coefficients" $U_n^j \in W$, $j = 1, \dots, k$, in the ansatz (4) :

$$\sum_{j=0}^k \alpha_{i,j} (U_n^j, v)_H = \frac{h_n}{2} \int_{\hat{I}} \left\langle F \left(\omega_n(\hat{t}), \sum_{j=0}^k U_n^j \hat{\phi}_j(\hat{t}) \right), v \right\rangle \hat{\psi}_i(\hat{t}) d\hat{t} \quad \forall v \in W \quad (8)$$

where $i = 0, \dots, k-1$,

$$\alpha_{i,j} := \int_{\hat{I}} d_i \hat{\phi}_j(\hat{t}) \hat{\psi}_i(\hat{t}) d\hat{t},$$

and the "coefficient" $U_n^0 \in W$ is known. We approximate the integral on the right hand side of (8) by the $(k+1)$ -point *Gauß-Lobatto quadrature formula*:

$$\int_{\hat{I}} \left\langle F \left(\omega_n(\hat{t}), \sum_{j=0}^k U_n^j \hat{\phi}_j(\hat{t}) \right), v \right\rangle \hat{\psi}_i(\hat{t}) d\hat{t} \approx \sum_{\mu=0}^k \hat{w}_\mu \left\langle F \left(\omega_n(\hat{t}_\mu), \sum_{j=0}^k U_n^j \hat{\phi}_j(\hat{t}_\mu) \right), v \right\rangle \hat{\psi}_i(\hat{t}_\mu),$$

where \hat{w}_μ are the weights and $\hat{t}_\mu \in [-1, 1]$ are the integration points with $\hat{t}_0 = -1$ and $\hat{t}_k = 1$. Let us define the mapped Gauß-Lobatto points $t_{n,\mu} \in \bar{I}_n$ and the coefficients $\beta_{i,\mu}, \gamma_{j,\mu}$ by

$$t_{n,\mu} := \omega_n(\hat{t}_\mu), \quad \beta_{i,\mu} := \hat{w}_\mu \hat{\psi}_i(\hat{t}_\mu), \quad \gamma_{j,\mu} := \hat{\phi}_j(\hat{t}_\mu).$$

Then, the system (8) is equivalent to the following system of equations for the k unknown "coefficients" $U_n^j \in W, j = 1, \dots, k$,

$$\sum_{j=0}^k \alpha_{i,j} (U_n^j, v)_H = \frac{h_n}{2} \sum_{\mu=0}^k \beta_{i,\mu} \left\langle F \left(t_{n,\mu}, \sum_{j=0}^k \gamma_{j,\mu} U_n^j \right), v \right\rangle \quad \forall v \in W. \quad (9)$$

with the k "equations" $i = 0, \dots, k-1$ where $U_n^0 = U_{n-1}^k$ for $n > 1$ and $U_1^0 = u_0$.

Once we have solved this system we enter the next time interval and set the initial value of the new time interval I_{n+1} to $U_{n+1}^0 := U_n^k$. If the Gauß-Lobatto formula would be exact for the right hand side of (8) this time marching process would solve the global time discretization (5) exactly. Since in general there is an integration error we call the time marching process corresponding to (9) simply the "cGP(k)-method".

In principle, we have to solve a coupled system for the $U_n^j \in W$ which could be very expensive. However, by a clever choice of the functions $\hat{\phi}_j$ and $\hat{\psi}_i$ it is possible to uncouple the system to a large extend. In the following, we will discuss this issue for the special methods cGP(1), cGP(2) and for the general method cGP(k), $k \geq 3$. In all cases, we choose the basis functions $\hat{\phi}_j \in \mathbb{P}_k(\hat{I})$ as the Lagrange basis functions with respect to the Gauß-Lobatto points \hat{t}_μ , i.e.,

$$\hat{\phi}_j(\hat{t}_\mu) = \delta_{j,\mu} \quad \forall j, \mu \in \{0, \dots, k\}.$$

Then, the method (9) reduces to

$$\sum_{j=0}^k \alpha_{i,j} (U_n^j, v)_H = \frac{h_n}{2} \sum_{j=0}^k \beta_{i,j} \langle F(t_{n,j}, U_n^j), v \rangle \quad \forall v \in W, \quad i = 0, \dots, k-1,$$

and by the choice of the test basis functions $\hat{\psi}_i \in \mathbb{P}_{k-1}(\hat{I})$ we try to get suitable values for the coefficients $\alpha_{i,j}$ and $\beta_{i,j}$. In the following, we will use the following abbreviation and assumption:

$$F_n^j(U_n^j) := F(t_{n,j}, U_n^j) \in H' \quad \forall j = 0, \dots, k, \quad n = 1, \dots, N. \quad (10)$$

2.1.1 The cGP(1) method

We use the 2-point Gauß-Lobatto formula (trapezoidal rule) with $\hat{w}_0 = \hat{w}_1 = 1$ and $\hat{t}_0 = -1, \hat{t}_1 = 1$. The only test function $\hat{\psi}_0$ is chosen as $\hat{\psi}_0(\hat{t}) = 1$. Then, we obtain

$$\alpha_{0,0} = -1, \quad \alpha_{0,1} = 1, \quad \beta_{0,0} = \beta_{0,1} = 1.$$

Using the notation $U^{n-1} := u_h(t_{n-1}) = U_n^0$ and $U^n := u_h(t_n) = U_n^1$, we obtain the following equation for the "unknown" $U^n \in W$:

$$(U^n, v)_H - (U^{n-1}, v)_H = \frac{h_n}{2} \{ \langle F(t_{n-1}, U^{n-1}) + F(t_n, U^n), v \rangle \}$$

for all $v \in W$ which is the well-known *Crank-Nicolson method*. In operator notation it can be written in the equivalent form:

$$U^n = U^{n-1} + \frac{h_n}{2} M^{-1} \{ F(t_{n-1}, U^{n-1}) + F(t_n, U^n) \}.$$

2.1.2 The cGP(2) method

We use the 3-point Gauß-Lobatto formula (Simpson rule) with $\hat{w}_0 = \hat{w}_2 = 1/3$, $\hat{w}_1 = 4/3$ and $\hat{t}_0 = -1, \hat{t}_1 = 0, \hat{t}_2 = 1$. For the test functions $\hat{\psi}_i \in \mathbb{P}_1(\hat{I})$, we choose

$$\hat{\psi}_0(\hat{t}) = -\frac{3}{4}\hat{t}, \quad \hat{\psi}_1(\hat{t}) = 1.$$

Then, we get

$$(\alpha_{i,j}) = \begin{pmatrix} -1/2 & 1 & -1/2 \\ -1 & 0 & 1 \end{pmatrix}, \quad (\beta_{i,j}) = \begin{pmatrix} 1/4 & 0 & -1/4 \\ 1/3 & 4/3 & 1/3 \end{pmatrix}$$

and the assumption (10), the system to compute the "unknowns" $U_n^1, U_n^2 \in W$ from the known $U_n^0 = U_{n-1}^2$ reads:

$$U_n^1 = \frac{1}{2}U_n^0 + \frac{1}{2}U_n^2 + \frac{h_n}{8}M^{-1} \{ F_n^0(U_n^0) - F_n^2(U_n^2) \} \quad (11)$$

$$U_n^2 = U_n^0 + \frac{h_n}{6}M^{-1} \{ F_n^0(U_n^0) + 4F_n^1(U_n^1) + F_n^2(U_n^2) \}. \quad (12)$$

Let us denote the value for U_n^1 computed from (11) and depending on U_n^2 by $U_n^1 = G_n^1(U_n^2)$ where $G_n^1 : W \rightarrow W$ in general is a nonlinear operator. We substitute this in the equation (12) and get, for the unknown $U_n^2 \in W$, the following fixed point equation:

$$U_n^2 = G_n^2(U_n^2) := U_n^0 + \frac{h_n}{6}M^{-1} \{ F_n^0(U_n^0) + 4F_n^1(G_n^1(U_n^2)) + F_n^2(U_n^2) \}$$

The mapping $G_n^2 : W \rightarrow W$ is a contraction if the time step size τ_n is sufficiently small.

2.2 Gauss implicit Runge-Kutta methods

For the general autonomous first order differential equations

$$y'(t) = f(y(t)), \quad (13)$$

where for system (1), we choose $y = \begin{pmatrix} p \\ q \end{pmatrix}$ and $f(y) = \begin{pmatrix} -\nabla_q V(q) \\ -\nabla_p T(q) \end{pmatrix}$. Runge-Kutta methods are defined as

$$y_{n+1} = y_n + h \sum_{i=1}^s b_i f(Y_i)$$

and

$$Y_i = y_n + h \sum_{j=1}^s a_{ij} f(Y_j)$$

where the coefficients a_{ij} , b_i and stage s determine the method. The Gauss methods have the highest possible order $r = 2s$ and are symplectic and symmetric. We exclusively consider $s = 2$, fourth order method for a fair comparison.

2.3 General linear methods

General linear methods provide numerical solutions of initial value problems of the form (13) A general linear method is of the form,

$$\begin{aligned} Y &= h(A \otimes I)f(Y) + (U \otimes I)y^{[n-1]}, \\ y^{[n]} &= h(B \otimes I)f(Y) + (V \otimes I)y^{[n-1]}. \end{aligned}$$

where $A \otimes I$ is the Kronecker product of the matrix A and the identity matrix I and h represents the step size. The s -component vector Y are the stages and $f(Y)$ are the stage derivatives. The vector $y^{[n-1]}$ with r -components is an input at the beginning of a step and results in output approximation $y^{[n]}$. With a slight abuse of notation, we can write,

$$\begin{aligned} Y &= hAf(Y) + Uy^{[n-1]}, \\ y^{[n]} &= hBf(Y) + Vy^{[n-1]}. \end{aligned}$$

The matrices A , U , V and B represent a particular general linear method and are generally displayed as,

$$\left[\begin{array}{c|c} A & U \\ \hline B & V \end{array} \right].$$

A fourth order symmetric G -symplectic general linear method is constructed with four stages ($s = 4$) and three input values ($r = 3$). The coefficients of the method are given in [10].

3 Numerical Experiments

We performed numerical comparisons of the continuous Galerkin Petrov time discretization scheme, general linear method and implicit Gauss R-K method

all having the same order four, for some Hamiltonian systems including simple harmonic oscillator, Kepler's problem with different eccentricities and molecular dynamical problems. Throughout the comparison, continuous Galerkin Petrov scheme is denoted by acronym cGP(2), while general linear method and implicit Gauss R-K method are represented by the acronym glm4 and irk4 respectively. The emphasis in our comparison is on the accuracy of solution, including the phase information, energy conservation and CPU time using above discussed methods. For each method and problem, we used different stepsizes and several intervals of integration. Stepsizes were chosen as a compromise between having small truncation error and performing efficient integration on each step. The accuracy of the solution was measured by the L_2 norm of the absolute global error in the position and velocity coordinates and is denoted by $E_g(t)$. The relative error in Hamiltonian is defined as

$$E_e(t) = \frac{E(t) - E(0)}{E(0)}.$$

Growth of global error is measured for first two problems as their exact solution exists, while relative error in Hamiltonian $E_e(t)$ is calculated for all problems. We also measured computational effort using the CPU time. All the comparisons are done on the same machine and are optimized using MATLAB.

Simple Harmonic Oscillator

As an example of simple harmonic oscillator a mass spring system having kinetic energy $p^2/(2m)$, where $p = mv$ is the momentum of the system and potential energy $\frac{1}{2}kq^2$. Where q is distance from the equilibrium, m is the mass of the body which is attached to spring and k is constant of proportionality often called as spring constant. Here the Hamiltonian is the total energy of the system and has one degree of freedom

$$H(q, p) = \frac{1}{2}kq^2 + \frac{p^2}{2m}.$$

The equations of motion from the Hamiltonian are

$$q' = \frac{\partial H(q, p)}{\partial p} = p, \quad p' = -\frac{\partial H(q, p)}{\partial q} = -q.$$

We compared the problem using different stepsizes of $h = 0.005, 0.01, 0.025,$ and 0.05 . Figure 1 gives the log-log graph for time versus global error $E_g(t)$ and relative error in Hamiltonian $E_e(t)$ using stepsize $h = 0.005$ for the time interval $[0, 1000]$. We found almost the same behavior of error growth for position and Hamiltonian using the rest of stepsizes. In Figure 1, the top plot gives the growth of global error and is approximately same for all tested methods, irk4 and cGP(2) having the least error while glm4 with slightly bigger error. In bottom plot of figure 1, the error in Hamiltonian is conserved by the methods. We also calculated the error growth according to Brouwer's law [12], our calculation shows that the exponent of time is 1 and 0.6 for $E_g(t)$ and $E_e(t)$ respectively, closed to its expected value. Table 1 gives the cost of integration for simple harmonic oscillator using all stepsizes. The table lists the stepsizes, maximum of global error, maximum of Hamiltonian error and CPU time. We observe from

Method	stepsize (h)	Max. of Global Error	Max. of Hamiltonian Error	CPU Time (sec.)
cGP(2)	0.05	8.67×10^{-6}	4.08×10^{-14}	2.8
cGP(2)	0.025	5.42×10^{-7}	1.07×10^{-13}	5.3
cGP(2)	0.01	1.38×10^{-8}	1.12×10^{-13}	12.1
cGP(2)	0.005	8.68×10^{-10}	1.31×10^{-13}	23.9
glm4	0.05	2.51×10^{-5}	4.67×10^{-11}	3.2
glm4	0.025	1.57×10^{-6}	7.57×10^{-13}	11.6
glm4	0.01	4.09×10^{-8}	3.1×10^{-15}	78.6
glm4	0.005	3.34×10^{-9}	1.14×10^{-15}	395.3
irk4	0.05	8.67×10^{-6}	6.43×10^{-15}	5.7
irk4	0.025	5.41×10^{-7}	2.51×10^{-14}	11.5
irk4	0.01	1.31×10^{-8}	1.97×10^{-14}	45.0
irk4	0.005	6.98×10^{-11}	3.68×10^{-14}	191.8

Table 1: Maximum of global error, Hamiltonian error and CPU time for simple harmonic oscillator.

the Table 1 that cGP(2) used the least CPU time and also having the least value for maximum of global error except for $h = 0.005$, where irk4 having the least end point global error, may be because of entering in a dip also depicted in Figure 1. The methods irk4 and glm4 are using eight and sixteen times more CPU time than cGP(2) giving similar accuracy for $h = 0.005$.

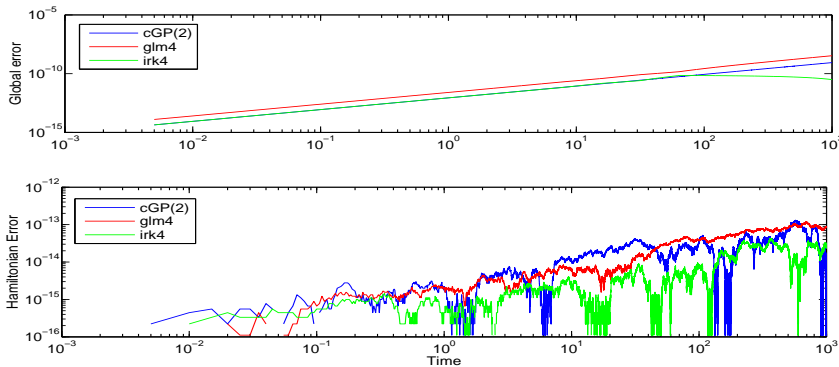


Figure 1: The growth of global error and relative error in Hamiltonian for Simple harmonic oscillator using stepsize $h = 0.005$.

Kepler's Problem

Kepler's problem is two body orbital problem in which the bodies are moving under their mutual gravitational forces. We can assume that one body is fixed at the origin and the second body is located in the plane with coordinates (q_1, q_2) . The solution of this problem is used in many important applications which includes the determination of orbits for new asteroids and the measurement of orbits for the two primary bodies in a restricted three body problem. The

Hamiltonian of the system can be written in separable form as [1]

$$H(q, p) = \frac{1}{2}(p_1^2 + p_2^2) - \frac{1}{\sqrt{q_1^2 + q_2^2}}$$

This can be written as $H = T + V$, where $T = (p_1^2 + p_2^2)/2$ and $V = -1/\sqrt{q_1^2 + q_2^2}$ are kinetic and potential energy of the system respectively. As like the previous problem, this system is also autonomous so the Hamiltonian H is a conserved quantity.

The equations of motion are

$$\begin{aligned} q_1' &= p_1, & q_2' &= p_2 \\ p_1' &= q_1'' = -\frac{q_1}{(q_1^2 + q_2^2)^{\frac{3}{2}}} \\ p_2' &= q_2'' = -\frac{q_2}{(q_1^2 + q_2^2)^{\frac{3}{2}}} \end{aligned} \tag{14}$$

with the initial conditions

$$q_1(0) = 1 - e, \quad q_2(0) = 0, \quad q_1'(0) = 0, \quad q_2'(0) = \sqrt{\frac{1+e}{1-e}}$$

where e is eccentricity $0 \leq e < 1$. The exact solution of the above equations (14) is

$$y_1 = \cos(E) - e, \quad y_2 = \sqrt{1 - e^2} \sin(E),$$

and

$$y_1' = -\sin(E)(1 - e \cos(E))^{-1}, \quad y_2' = \sqrt{(1 - e^2)} \cos(E)(1 - e \cos(E))^{-1},$$

where the eccentric anomaly E satisfies Kepler's equation $t = E - e \sin(E)$. Since Kepler's equation is implicit in E , the equation is usually solved using a non-linear equation solver, although useful analytical approximations can be found for smaller eccentricity.

The integrations are performed for Kepler's problem with different eccentricities $e = 0, 0.5$ and 0.9 . The integration is done for 1000 periods for $e = 0$ and 100 periods for $e = 0.5$ and 0.9 . For each method, we measured $E_y(t)$ and $E_e(t)$ throughout the interval of integration. A variety of different stepsizes are used to analyze the behaviour of error growth. We used the stepsizes of $h = \frac{2\pi}{400}$, $h = \frac{2\pi}{800}$, $h = \frac{2\pi}{1600}$, $h = \frac{2\pi}{3200}$ and $h = \frac{2\pi}{6400}$ for eccentricities $e = 0, 0.5$ and 0.9 . A log-log plot of time against error is given for Kepler's problem in Figures 2 and 3 using eccentricities 0 and 0.9 respectively. Growth of errors in both quantities behave in the same manner as for $e=0.5$. It is seen that the global error growth is approximately linear for cGP(2), irk4 and glm4, i. e., growing as $t^{0.9}$ (see figures 2 and 3). The error in Hamiltonian remains conserved for cGP(2), irk4 and glm4 for the intervals of integration. Our calculation shows that for $E_e(t)$ grows as $t^{0.6}$, showing a good agreement to its expected value. The cGP(2) exhibits a smaller error even the problem becomes more eccentricitic (see Figures 2 and 3).

We also measured the cost of integration for Kepler's problem using all stepsizes for all three eccentricities. Tables 2, 3 and 4 lists the stepsizes,

Method	stepsize (h)	Max. of Global Error	Max. of Hamiltonian Error	CPU Time (sec.)
cGP(2)	$2\pi/400$	4.88×10^{-6}	4.07×10^{-13}	93.4
cGP(2)	$2\pi/800$	2.54×10^{-7}	7.54×10^{-12}	192.7
cGP(2)	$2\pi/1600$	6.56×10^{-8}	1.28×10^{-11}	378
cGP(2)	$2\pi/3200$	1.38×10^{-8}	2.28×10^{-12}	760.5
cGP(2)	$2\pi/6400$	4.54×10^{-9}	1.49×10^{-12}	1487
glm4	$2\pi/400$	2.36×10^{-5}	2.35×10^{-14}	3464
glm4	$2\pi/800$	1.56×10^{-6}	3.06×10^{-14}	12172
glm4	$2\pi/1600$	1.66×10^{-7}	9.39×10^{-14}	47724
glm4	$2\pi/3200$	8.59×10^{-8}	5.32×10^{-13}	180716
glm4	$2\pi/6400$	1.05×10^{-8}	9.98×10^{-12}	752864
irk4	$2\pi/400$	1.04×10^{-5}	4.72×10^{-14}	1598
irk4	$2\pi/800$	5.68×10^{-7}	2.79×10^{-14}	6348
irk4	$2\pi/1600$	2.98×10^{-7}	3.28×10^{-14}	23609
irk4	$2\pi/3200$	6.58×10^{-8}	5.17×10^{-13}	93215
irk4	$2\pi/6400$	1.27×10^{-8}	7.18×10^{-12}	39460

Table 2: Maximum of global error, Hamiltonian error and CPU time for Kepler's Problem with $e = 0$ for 10^3 periods.

maximum of global error, maximum of Hamiltonian error and CPU time for $e = 0, e = 0.5$ and 0.9 respectively. We observe from the information depicted in tables, that cGP(2) used the least CPU time and also having the least value for maximum of global error for all the stepsizes. For $e=0$, using the least stepsize i.e $h = \frac{2\pi}{6400}$, irk4 and glm4 used 506 and 26 times more CPU time than cGP(2). While for $e=0.5$ and 0.9 , irk4 and glm4 used nearly 55 and 24 times more CPU time than cGP(2).

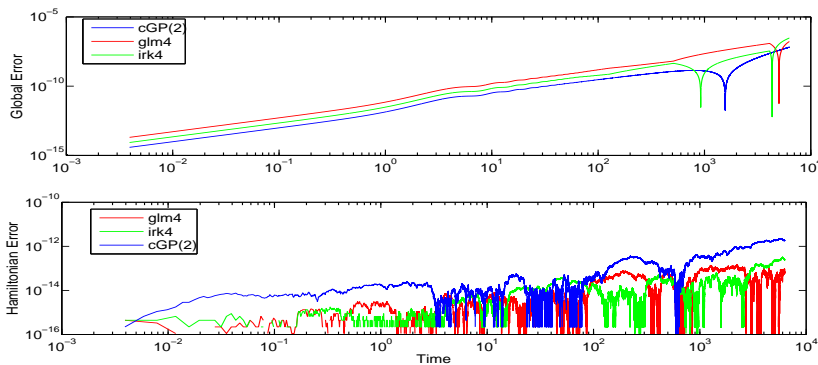


Figure 2: The growth of global error and relative error in Hamiltonian for Kepler's problem with $e = 0$ using stepsize $2\pi/6400$ for 10^3 periods.

Method	stepsize (h)	Max. of Global Error	Max. of Hamiltonian Error	CPU Time (sec.)
cGP(2)	$2\pi/400$	1.06×10^{-4}	2.83×10^{-8}	10.2
cGP(2)	$2\pi/800$	6.63×10^{-6}	1.77×10^{-9}	19.9
cGP(2)	$2\pi/1600$	4.15×10^{-7}	1.11×10^{-10}	39.8
cGP(2)	$2\pi/3200$	2.54×10^{-8}	7.01×10^{-12}	79.2
cGP(2)	$2\pi/6400$	2.9×10^{-9}	1.02×10^{-12}	157.5
glm4	$2\pi/400$	2.1×10^{-4}	5.97×10^{-8}	43.8
glm4	$2\pi/800$	1.31×10^{-5}	3.74×10^{-9}	182.3
glm4	$2\pi/1600$	8.2×10^{-7}	2.34×10^{-10}	688.2
glm4	$2\pi/3200$	3.31×10^{-8}	1.46×10^{-11}	2366
glm4	$2\pi/6400$	2.16×10^{-8}	1.38×10^{-12}	8789
irk4	$2\pi/400$	8.84×10^{-5}	1.89×10^{-8}	22.1
irk4	$2\pi/800$	5.53×10^{-6}	1.18×10^{-9}	68.5
irk4	$2\pi/1600$	3.43×10^{-7}	4.71×10^{-11}	244
irk4	$2\pi/3200$	1.04×10^{-8}	4.66×10^{-12}	955
irk4	$2\pi/6400$	2.51×10^{-8}	3.13×10^{-13}	3830

Table 3: Maximum of global error, Hamiltonian error and CPU time for Kepler's Problem with $e = 0.5$ for 10^2 periods.

Method	stepsize (h)	Max. of Global Error	Max. of Hamiltonian Error	CPU Time (sec.)
cGP(2)	$2\pi/400$	4.87	5.23×10^{-3}	10.4
cGP(2)	$2\pi/800$	1.68	2.43×10^{-4}	20.2
cGP(2)	$2\pi/1600$	1.92×10^{-1}	1.42×10^{-5}	41.1
cGP(2)	$2\pi/3200$	1.3×10^{-2}	8.74×10^{-7}	80.6
cGP(2)	$2\pi/6400$	8.41×10^{-6}	5.43×10^{-8}	162.1
glm4	$2\pi/400$	111.8	6.5×10^{-4}	44.1
glm4	$2\pi/800$	4.54	2.23×10^{-4}	172
glm4	$2\pi/1600$	1.46	1.62×10^{-5}	676
glm4	$2\pi/3200$	9.77×10^{-2}	1.04×10^{-6}	2482
glm4	$2\pi/6400$	6.14×10^{-3}	6.53×10^{-8}	8402
irk4	$2\pi/400$	4.54	1.73×10^{-5}	22.4
irk4	$2\pi/800$	1.27	1.36×10^{-5}	67.8
irk4	$2\pi/1600$	1.32×10^{-1}	1.38×10^{-6}	257.5
irk4	$2\pi/3200$	9.01×10^{-3}	9.45×10^{-8}	1086
irk4	$2\pi/6400$	5.73×10^{-4}	6.03×10^{-9}	3786

Table 4: Maximum of global error, Hamiltonian error and CPU time for Kepler's Problem with $e = 0.9$ for 10^2 periods.

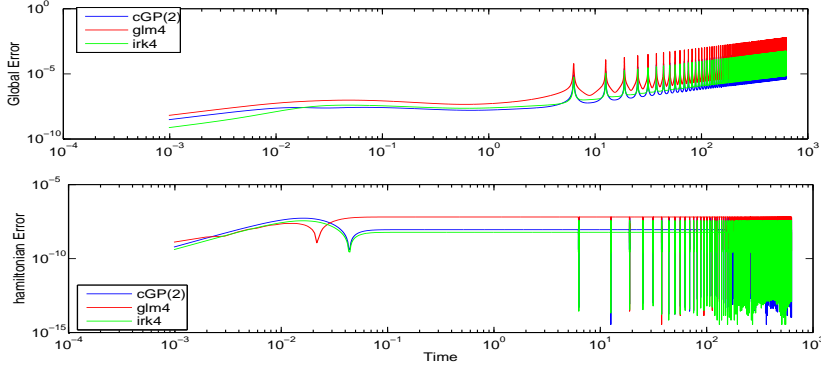


Figure 3: The growth of global error and relative error in Hamiltonian for kepler's problem with $e = 0.9$ using stepsize $2\pi/1600$ for 10^2 periods.

Molecular Dynamical Problem

We consider the interaction of seven Argon atoms in two dimension, where one of the atom is centered by six atoms which are symmetrically arranged [13]. The Hamiltonian for the molecular dynamics is written as [1]

$$H(q, p) = \frac{1}{2} \sum_{i=1}^7 \frac{1}{m_i} p_i^T p_i + \sum_{i=2}^7 \sum_{j=1}^{i-1} V_{ij} \|q_i - q_j\|$$

where $V_{ij}(r)$ are potential functions. Here q_i and p_i are positions and generalized momenta for the atoms. And m_i denotes the atomic mass of the i th atom.

$$V_{ij}(r) = 4\varepsilon_{ij} \left(\left(\frac{\sigma_{ij}}{r} \right)^{12} - \left(\frac{\sigma_{ij}}{r} \right)^6 \right).$$

The equations of motion for the frozen Argon crystals are given as

$$q_i''(t) = \frac{24\varepsilon\sigma^6}{m_i} \sum_{j=1, j \neq i}^7 \left[\frac{(q_j - q_i)}{\|q_j - q_i\|_2^8} - 2\sigma^6 \frac{(q_j - q_i)}{\|q_j - q_i\|_2^{14}} \right], \quad i = 1, \dots, 7,$$

where $r = \sigma_{ij} \sqrt[6]{2}$, $m_i = 66.34 \times 10^{-27} [\text{kg}]$, $\sigma_{ij} = \sigma = 0.341 [\text{nm}]$ and $\varepsilon = 1.654028284 \times 10^{-21} [\text{J}]$. Initial positions and initial velocities are taken in [nm] and [nm/sec] respectively [1].

In molecular dynamics, since much interest is emphasized on macroscopic quantities like Hamiltonian. So we also discussed only the energy conservation of atoms over an interval of length 2×10^5 [fsec] ($1 \text{fsec} = 10^{-6}$). The experiments are done using the stepsizes of 0.5 fsec, 1 fsec, 2 fsec and 4 fsec. The graphical results are only shown for $h = 0.5 \times 10^{-6} [\text{fsec}]$ as the error growth using other stepsizes was approximately same. Figure 4 shows that the tested methods conserve the value of Hamiltonian H even though the conservation is of highly oscillatory, while the error in Hamiltonian for cGP(2) grows as $t^{0.7}$. On the other hand, for irk4 and glm4 the exponent of time is 0.59 and 0.61 respectively. Table 5 gives the cost of integration for molecular dynamical problem using

Method	stepsize (h)	Max. of Global Error	CPU Time (sec.)
cGP(2)	4	1.24×10^{-9}	658
cGP(2)	2	6.15×10^{-11}	1323
cGP(2)	1	7.05×10^{-12}	2680
cGP(2)	0.5	3.73×10^{-13}	5821
glm4	4	9.24×10^{-11}	1772
glm4	2	5.58×10^{-12}	4300
glm4	1	3.53×10^{-13}	11367
glm4	0.5	9.41×10^{-14}	34591
irk4	4	3.72×10^{-11}	2060
irk4	2	2.32×10^{-12}	4272
irk4	1	1.59×10^{-13}	10020
irk4	0.5	2.34×10^{-14}	23596

Table 5: Maximum of Hamiltonian error and CPU time for molecular dynamical problem for 2×10^5 [fsec].

all stepsizes. The table lists the stepsizes, maximum of Hamiltonian error and CPU time. It is observed from the Table 5 that cGP(2) used the least CPU time for all the stepsizes used but exhibiting slightly big maximum of Hamiltonian error. The methods irk4 and glm4 having almost the same error growth for the integrated interval.

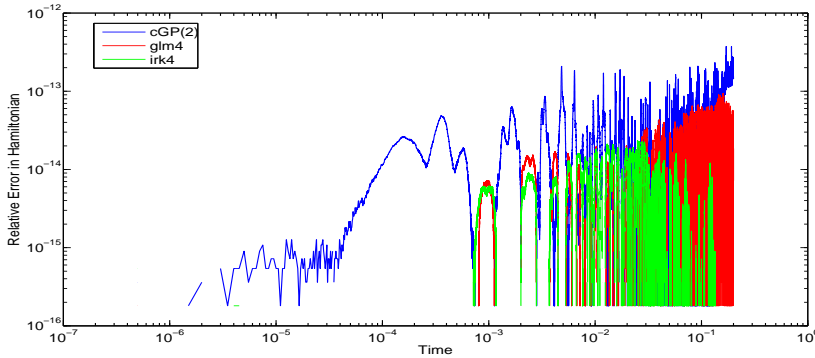


Figure 4: The growth of relative error in Hamiltonian using $h = 0.5 \times 10^{-6}$ [fsec] for molecular dynamical problem over an interval of 2×10^5 [fsec].

4 Summary

We implemented and analyzed the cGP(2) for Hamiltonian systems such as harmonic oscillator, Kepler's problem and molecular dynamical problem. The obtained results are also compared with symplectic methods irk4 and glm4. It is shown that the cGP(2) method conserves the hamiltonian as other tested symplectic methods do. Moreover, giving the efficiency approximately same

as other methods yield, cGP(2) uses marginally less CPU time than compared methods.

References

- [1] Hairer, E., Lubich, C., Wanner, G. Geometric Numerical Integration, Springer-Verlag, Berlin, Heidelberg Germany, 2006.
- [2] Eirola, T. and Sanz-Serna, J.M. Conservation of integrals and symplectic structure in the integration of differential equations by multistep methods, *Numer. Math.*, 61:281-290, 1992.
- [3] Hairer, E. Conjugate-symplecticity of linear multistep methods, *J. Comput. Math.*, 26(5):657–659, 2008.
- [4] Sanz-Serna, J. M., Calvo, M. P. Numerical Hamiltonian Problems, Chapman and Hall, Great Britain, 1994.
- [5] Schieweck, F. A-stable discontinuous Galerkin-Petrov time discretization of higher order. *J. Numer. Math.*, 18(1):25–57, 2010.
- [6] Hussain, S., Schieweck, F. and Turek, S. Higher order Galerkin time discretizations and fast multigrid solvers for the heat equation. *J. Numer. Math.*, 19(1):4161, 2011.
- [7] Aziz, A. K. and Monk, P. Continuous finite elements in space and time for the heat equation. *Math. Comp.*, 52(186):255-274, 1989.
- [8] Thomee, V. Galerkin finite element methods for parabolic problems, volume 25 of Springer Series in Computational Mathematics. Springer-Verlag, Berlin, second edition, 2006.
- [9] Butcher, J. C. Numerical Methods for Ordinary Differential Equations, John Wiley and Sons, Ltd, 2008.
- [10] Butcher, J. C., Habib, Y., Hill, A. T. and Norton, T. J. T. The control of parasitism in G-symplectic methods, *SIAM J. Numer. Anal.*, 52(5):2440–2465, 2014.
- [11] Habib, Y. Long-Term Behaviour of G-symplectic Methods, PhD Thesis, The University of Auckland, 2010. <https://researchspace.auckland.ac.nz/handle/2292/6641>
- [12] Brouwer D. On the accumulation of errors in numerical integration. *Astron. J.*, 46:149-153, 1937
- [13] Biesiadecki, J. J. and Skeel, R. D. Dangers of multiple time step methods, *J. Comput. Phys.* 109,1993, 318-328. [I.4], [VIII.4], [XIII.1]